

A MODIFIED IMPULSE CONTROLLER FOR IMPROVED ACCURACY OF ROBOTS WITH FRICTION

Stephen van Duin, Christopher D. Cook, Zheng Li and Gursel Alici
Faculty of Engineering, University of Wollongong, Northfields Avenue, Gwynnville, Australia

Keywords: Impulsive control, static friction, limit cycle, stick-slip, impulse shape, friction model, accuracy.

Abstract: This paper presents a modified impulse controller to improve the steady state positioning of a SCARA robot having characteristics of high non-linear friction. A hybrid control scheme consisting of a conventional PID part and an impulsive part is used as a basis to the modified controller. The impulsive part uses short width torque pulses to provide small impacts of force to overcome static friction and move a robot manipulator towards its reference position. It has been shown that this controller can greatly improve a robot's accuracy. However, the system in attempting to reach steady state will inevitably enter into a small limit cycle whose amplitude of oscillation is related to the smallest usable impulse. It is shown in this paper that by modifying the impulse controller to adjust the width of successive pulses, the limit cycle can be shifted up or down in position so that the final steady state error can be even further reduced.

1 INTRODUCTION

Precision robot manufacturers continually strive to increase the accuracy of their machinery in order to remain competitive. The ability of a robot manipulator to position its tool centre point to within a very high accuracy, allows the robot to be used for more precise tasks. For positioning of a tool centre point, the mechanical axes of a robot will be required to be precisely controlled around zero velocity where friction is highly non-linear and difficult to control.

Non-linear friction is naturally present in all mechanisms and can cause stick-slip during precise positioning. In many instances, stick-slip has been reduced or avoided by modifying the mechanical properties of the system; however this approach may not always be practical or cost effective. Alternatively, advances in digital technology have made it possible for the power electronics of servomechanisms to be controlled with much greater flexibility. By developing better controllers, the unfavourable effects of non-linear friction may be reduced or eliminated completely.

Impulse control has been successfully used for accurate positioning of servomechanisms with high friction where conventional control schemes alone have difficulty in approaching zero steady state

error. Static and Coulomb friction can cause a conventional PID controller having integral action (I), to overshoot and limit cycle around the reference position. This is a particular problem near zero velocities where friction is highly non linear and the servomechanism is most likely to stick-slip. Despite the above difficulties, PID controllers are still widely used in manufacturing industries because of their robustness to parameter uncertainty and unknown disturbances.

Stick-slip can be reduced or eliminated by using impulsive control near or at zero velocities. The impulsive controller is used to overcome static friction by impacting the mechanism and moving it by microscopic amounts. By combining the impulsive controller and conventional controller together, the PID part can be used to provide stability when moving towards the reference position while the impulse controller is used to improve accuracy for the final positioning where the error signal is small.

By applying a short impulse of sufficient force plastic deformation occurs between the asperities of mating surfaces resulting in permanent controlled movement. If the initial pulse causes insufficient movement, the impulsive controller produces additional pulses until the position error is reduced to a minimum.

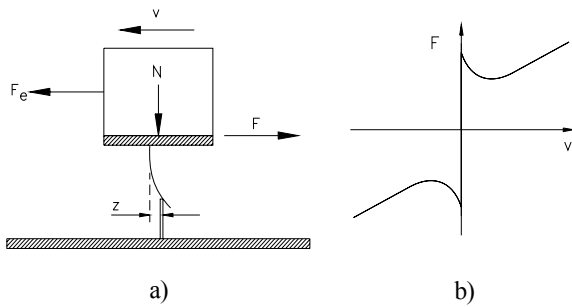


Figure 1: Bristle model; Figure a) shows the deflection of a single bristle. Figure b) shows the resulting static friction model for a single instance in time.

A number of investigators have devised impulsive controllers which achieve precise motion in the presence of friction by controlling the height or width of a pulse. Yang and Tomizuka (Yang et al, 1988) applied a standard rectangular shaped pulse whereby the height of the pulse is a force about 3 to 4 times greater than the static friction to guarantee movement. The width of the pulse is adaptively adjusted proportional to the error and is used to control the amount of energy required to move the mechanism towards the reference positioning. Alternatively, Popovic (Popovic et al, 2000) described a fuzzy logic pulse controller that determines both the optimum pulse amplitude and pulse width simultaneously using a set of membership functions. Hojjat and Higuchi (Hojjat et al, 1991) limited the pulse width to a fixed duration of 1ms and vary the amplitude by applying a force about 10 times the static friction. Rathbun et al (Rathbun et al, 2004) identify that a flexible-body plant can result in a position error limit cycle and that this limit cycle can be eliminated by reducing the gain using a piecewise-linear-gain pulse width control law.

In a survey of friction controllers by Armstrong-Hélouvry (Armstrong- Hélouvry et al, 1994), it is commented that underlying the functioning of these impulsive controllers is the requirement for the mechanism to be in the stuck or stationary position before subsequent impulses are applied. Thus, previous impulse controllers required each small impacting pulse to be followed by an open loop slide ending in a complete stop.



Figure 2: The Hirata SCARA robot.

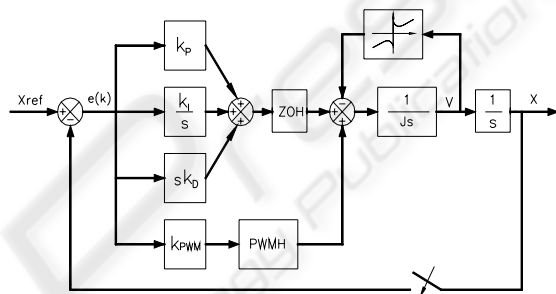


Figure 3: Block diagram of the experimental system controller.

In this paper, a hybrid PID + Impulsive controller is used to improve the precision of a servomechanism under the presence of static and Coulomb friction. The design and functioning of the controller does not require the mechanism to come to rest between subsequent pulses, making it suitable for both point to point positioning and speed regulation. The experimental results of this paper show that the shape of the impulse can be optimised to increase the overall precision of the controller. It is shown that the smallest available movement of the servomechanism can be significantly reduced without modification to the mechanical plant.

2 MODELLING AND EXPERIMENTAL SYSTEM

2.1 Friction Model

On a broad scale, the properties of friction are both well understood and documented. Armstrong-Hélouvry (Armstrong- Hélouvry et al, 1994) have surveyed some of the collective understandings of how friction can be modelled to include the

complexities of mating surfaces at a microscopic level. Canudas de Wit (Canudas de Wit et al, 1995) add to this contribution by presenting a new model that more accurately captures the dynamic phenomena of rising static friction (Rabinowicz, 1958), frictional lag (Rabinowicz, 1958), varying break away force (Johannes et al, 1973), (Richardson et al, 1976), dwell time (Kato et al, 1972), pre-sliding displacement (Dahl, 1968), (Dahl, 1977), (Johnson, 1987) and Stribeck effect (Olsson, 1996). The friction interface is thought of as a contact between elastic bristles. When a tangential force is applied, the bristles deflect like springs which give rise to the friction force (Canudas de Wit et al, 1995); see Figure 1(a). If the effective applied force F_e exceeds the bristles force, some of the bristles will be made to slip and permanent plastic movement occurs between each of the mating surfaces. The set of equations governing the dynamics of the bristles are given by (Olsson, 1996):

$$\frac{dz}{dt} = v - \frac{|v|}{g(v)} z \quad (1)$$

$$g(v) = \frac{1}{\sigma_0} \left(F_C + (F_s - F_C) e^{-(v/v_s)^2} \right) \quad (2)$$

$$F = \sigma_0 z + \sigma_1(v) \frac{dz}{dt} + F_v v \quad (3)$$

$$\sigma_1(v) = \sigma_1 e^{-(v/v_d)^2} \quad (4)$$

where v is the relative velocity between the two surfaces and z is the average deflection of the bristles. σ_0 is the bristle stiffness and σ_1 is the bristle damping. The term v_s is used to introduce the velocity at which the Stribeck effect begins while the parameter v_d determines the velocity interval around zero for which the velocity damping is active. Figure 1(b) shows the friction force as a function of velocity. F_s is the average static friction while F_C is the average Coulomb friction. For very low velocities, the viscous friction F_v is negligible but is included for model completeness. F_s , F_C , and F_v are all estimated experimentally by subjecting a real mechanical system to a series of steady state torque responses. The parameters σ_0 , σ_1 , v_s and v_d are also determined by measuring the steady state friction force when the velocity is held constant (Canudas de Wit et al, 1995).

2.2 Experimental System

For these experiments, a Hirata ARi350 SCARA (Selective Compliance Assembly Robot Arm) robot was used. The Hirata robot has four axes named A, B, Z and W. The main rotational axes are A-axis (radius 350mm) and B-axis (radius 300mm) and they control the end-effector motion in the horizontal plane. The Z-axis moves the end-effector in the vertical plane with a linear motion, while the W-axis is a revolute joint and rotates the end effector about the Z-axis. A photograph of the robot is shown in Figure 2.

For these experiments, only the A and B axis of the Hirata robot are controlled. Both the A and B axes have a harmonic gearbox between the motor and robot arm. Their gear ratios are respectively 100:1 and 80:1. All of the servomotors on the Hirata robot are permanent magnet DC type and the A and B axis motors are driven with Baldor® TSD series DC servo drives. Each axis has characteristics of high non-linear friction whose parameters are obtained by direct measurement. For both axes, the static friction is approximately 1.4 times the Coulomb friction.

Matlab's xPC target oriented server was used to provide control to each of the servomotor drives. For these experiments, each digital drive was used in current control mode which in effect means the output voltage from the 12-bit D/A converter gives a torque command to the actuator's power electronics. The system controller was compiled and run using Matlab's real time xPC Simulink® block code. A 12-bit A/D converter was used to read the actuator's shaft encoder position signal.

2.3 PID + Impulse Hybrid Controller

Figure 3 shows the block diagram of a PID linear controller + impulsive controller. This hybrid controller has been suggested by Li (Li et al, 1998) whereby the PID driving torque and impulsive controller driving torque are summed together. It is unnecessary to stop at the end of each sampling period and so the controller can be used for both position and speed control.

The controller can be divided into two parts; the upper part is the continuous driving force for large scale movement and control of external force disturbances. The lower part is an additional proportional controller k_{pwm} with a pulse width modulated sampled-data hold (PWMH), and is the basis of the impulsive controller for the control of stick-slip.

The system controller is sampled at 2 kHz. The impulse itself is sampled and applied at one twentieth of the overall sampling period (i.e. 100 Hz) to match the mechanical system dynamics. Figure 4 shows a typical output of the hybrid controller for one impulse sampling period τ_s . The pulse with height f_p is added to the PID output. Because the PID controller is constantly active, the

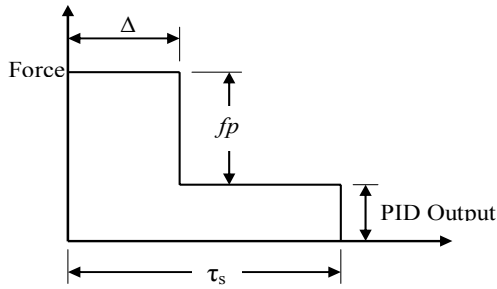


Figure 4: Friction controller output.

system has the ability to counteract random disturbances applied to the servomechanism. The continuous part of the controller is tuned to react to large errors and high velocity, while the impulse part is optimized for final positioning where stiction is most prevalent.

For large errors, the impulse width approaches the full sample period τ_s , and for very large errors, it transforms into a continuous driving torque. When this occurs, the combined control action of the PID controller and the impulsive controller will be continuous. Conversely, for small errors, the PID output is too small to have any substantial effect on the servomechanism dynamics.

The high impulse sampling rate, combined with a small error, ensures that the integral (I) part of the PID controller output has insufficient time to rise and produce limit cycling. To counteract this loss of driving torque, when the error is below a threshold, the impulsive controller begins to segment into individual pulses of varying width and becomes the primary driving force. One way of achieving this is to make the pulse width Δ determined by:

$$\Delta = \frac{k_{pwm} \cdot e(k) \tau_s}{f_p} \quad \text{if } k_{pwm} \cdot |e(k)| \leq f_p$$

$$\Delta = \tau_s \quad \text{otherwise} \quad (6)$$

In (6)

$$f_p = |f_p| \cdot \text{sign}(e(k)) \quad (7)$$

where $e(k)$ is the error input to the controller, $|f_p|$ is a fixed pulse height greater than the highest static friction and τ_s is the overall sampling period. For the experimental results of this paper, the impulsive sampling period τ_s was 10ms and the pulse width could be incrementally varied by 1ms intervals. The pulse width gain k_{pwm} , is experimentally determined by matching the mechanism's observed displacement d to the calculated pulse width t_p using the equation of motion:

$$d = \frac{f_p (f_p - f_c)}{2mf_c} t_p^2, \quad f_p > 0 \quad (8)$$

The gain is iteratively adjusted until the net displacement for each incremental pulse width is as small as practical.

2.4 Minimum Pulse Width

The precision of the system is governed by the smallest incremental movement which will be produced from the smallest usable width pulse. Because the shape of the pulse is affected by the system's electrical circuit response, a practical limit is placed on the amplitude of the pulse over very short durations and this restricts the amount of energy that can be contained within a very thin pulse. Consequently, there exists a minimum pulse width that is necessary to overcome the static friction and guarantee plastic movement.

For the Hirata robot, the minimum pulse width guaranteeing plastic displacement was determined to be 2ms and therefore the pulse width is adjusted between 2 and 10ms. Any pulse smaller than 2ms results in elastic movement of the mating surfaces in the form of pre-sliding displacement. In this regime, short impulses can produce unpredictable displacement or even no displacement at all. In some cases, the mechanism will spring back greater than the forward displacement resulting in a larger error. Figure 5 shows the displacement of the experimental system of five consecutive positive impulses followed by five negative impulses. The experiment compares impulses of width 2ms and 1.5ms. For impulses of 2ms, the displacement is represented by the consistent staircase movement. For a width of 1.5ms, the displacement is unpredictable with

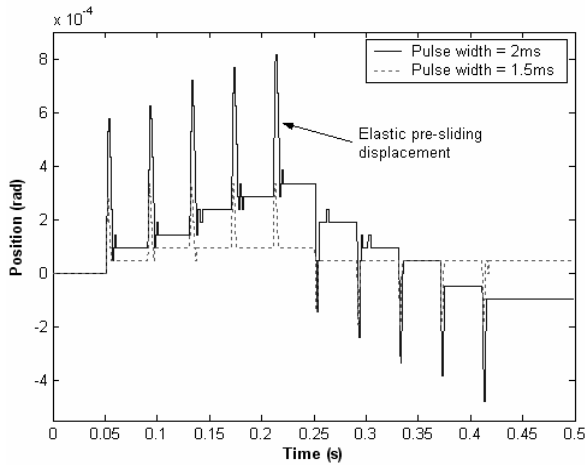


Figure 5: Experimentally measured displacement for both positive and negative impulses using successive pulse widths 1.5ms and 2ms.

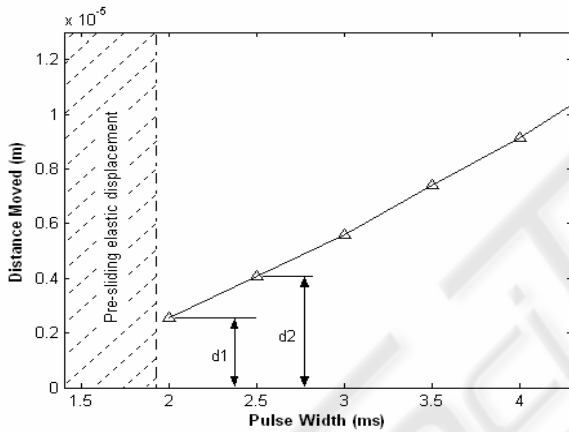


Figure 6: Simulated displacements as a function of pulse width.

mostly elastic pre-sliding movement which results in zero net displacement.

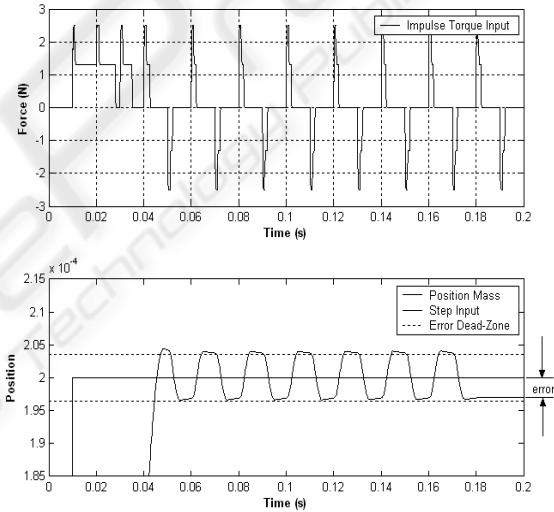
Wu et al (Wu et al, 2004) use the pre-sliding displacement as a means to increase the precision of the controller by switching the impulse controller off and using a continuous ramped driving torque to hold the system in the desired position. The torque is maintained even after the machine is at rest. This is difficult in practice as pre-sliding movement must be carefully controlled in the presence of varying static friction so that inadvertent breakaway followed by limit cycling is avoided.

3 LIMIT CYCLE OFFSET

3.1 Motivation

Figure 6 shows the simulated displacements of varying pulse widths which have been labelled $d1, d2, d3...dn$ respectively, where $d1$ is the minimum pulse width which will generate non elastic movement and defines the system's resolution.

Using the variable pulse width PID + impulse controller for a position pointing task, the torque will incrementally move the mechanism towards the reference set point in an attempt to reach steady state. Around the set point, the system will inevitably begin to limit cycle when the error $e(k)$ is approximately the same magnitude as the system resolution (the displacement for the minimum pulse width $d1$).



Parameter	F_s	F_C	σ_0	σ_I	F_V	v_s	v_d
Value	2	1	$4.5 \cdot 10^5$	12,000	0.4	0.001	0.0004

Figure 7: Simulation of the impulse controller limit cycling around a position reference set-point where the final torque output is a pulse with a minimum width and the mean peak to peak oscillation is $d1$. The friction parameters used for the simulation are also given in the accompanying table.

For the limit cycle to be extinguished, the controller must be disabled. As an example, the limit cycle in Figure 7 is extinguished by disabling the impulse controller at $t=0.18s$, and in this case, the resulting error is approximately half the displacement of the minimum pulse width $d1$.

Limit cycling will occur for all general servomechanisms using a torque pulse because every practical system inherently has a minimum pulse width that defines the system's resolution. Figure 7 simulates a typical limit cycle with a peak to peak oscillation equal to the displacement of the minimum pulse width $d1$.

One way to automatically extinguish the limit cycle is to include a dead-zone that disables the controller output when the error is between an upper and lower bound of the reference point (see Figure 7). The final error is then dependent on the amount of offset the limit cycle has in relation to the reference point. Figure 7 shows a unique case where the \pm amplitude of the limit cycle is almost evenly distributed either side of the reference set point; i.e. the centre line of the oscillation lies along the reference set point. In this instance, disabling the controller would create an error $e(k)$ equal to approximately $\left| \frac{d1}{2} \right|$. This however, would vary in practice and the centreline is likely to be offset by some arbitrary amount. The maximum precision of the system will therefore be between $d1$ and zero.

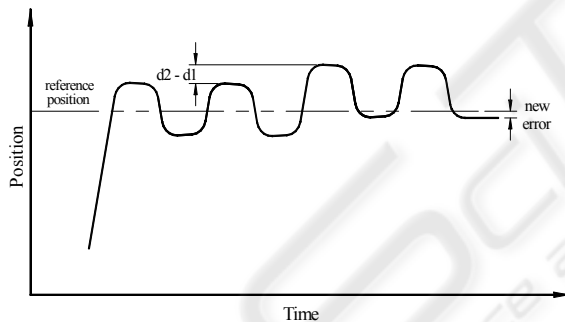


Figure 8: Conceptual example of reducing the steady state error using 'Limit Cycle Offset' with the limit cycle shifted up by $d2-d1$ and the new error that is guaranteed to fall within the dead-zone.

3.2 Limit Cycle Offset Function

By controlling the offset of the limit cycle centreline, it is possible to guarantee that the final error lies within the dead-zone, and therefore to increase the precision of the system. As a conceptual example, Figure 8 shows a system limit cycling either side of the reference point by the minimum displacement $d1$. By applying the next smallest pulse $d2$, then followed by the smallest pulse $d1$, the limit cycle can be shifted by $d2 - d1$. The effect is

that the peak to peak centreline of the oscillation has now been shifted away from the reference point.

However, at least one of the peaks of the oscillation has been shifted closer to the set point. If the controller is disabled when the mechanism is closest to the reference set point, a new reduced error is created. For this to be realised, the incremental difference in displacement between successively increasing pulses must be less than the displacement from the minimum pulse width; for example $d2 - d1 < d1$.

3.3 Modified Controller Design

For the limit cycle to be offset at the correct time, the impulse controller must have a set of additional control conditions which identify that a limit cycle has been initiated with the minimum width pulse. The controller then readjusts itself accordingly using a 'switching bound' and finally disables itself when within a new specified error 'dead-zone'. One way to achieve this is to adjust the pulse width so that it is increased by one increment when satisfying the following conditions:

if $switching\ bound > |e(k)| \geq dead-zone$

$$\text{then } \Delta = \frac{k_{pwm} \cdot e(k) \tau_s}{f_p} + 1$$

$$\text{otherwise } \Delta = \frac{k_{pwm} \cdot e(k) \tau_s}{f_p} \quad (9)$$

where the switching bound is given by:

$$|switching\ bound| < \frac{d1}{2} \quad (10)$$

and the dead-zone is given by:

$$|dead-zone| = \frac{(d2 - d1)}{2} \quad (11)$$

The steady state error $e(k)$ becomes:

$$|e(k)_{steady\ state}| \leq \frac{deadzone}{2} \quad (12)$$

3.4 Simulation of the Limit Cycle Offset Function

To demonstrate the limit cycle offset function, the modified controller is simulated using a simple unit mass with the ‘new’ friction model using Eqs. 1 to 4.

A simulated step response is shown in Figure 9 to demonstrate how the modified controller works. Here the mechanism moves towards the reference set point and begins limit cycling. Because at least

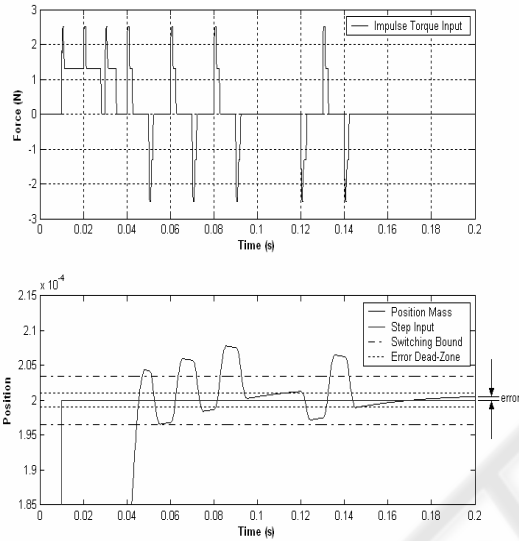


Figure 9: Simulation of the limit cycle offset function used with the PID + impulse controller.

one of the peaks of the limit cycle immediately lies within the switching bound, the controller shifts the peak to peak oscillation by $d2 - d1$ by applying the next smallest pulse, and then followed by the smallest pulse. In this example, the first shift is insufficient to move either peak into the set dead-zone so the controller follows with a second shift. At time 0.1 seconds, the controller is disabled; however, the elastic nature of the friction model causes the mechanism’s position to move out of the dead-zone. As a result, the controller is reactivated (time 0.12s) and the controller follows with a third shift. In this instance, the mechanism reaches steady state at $t=0.2s$, and the final error is $|e(k)| \leq \frac{1}{2} \cdot (\text{dead zone})$ which in this case is $\pm 1e-6$ radians. A final analysis of the result shows that the new controller has reduced the error by an amount significantly more than a standard impulse controller. This reduction correlates directly to the

improvement in the system’s accuracy by a factor of 4.

4 EXPERIMENTAL

4.1 Position Pointing

This section evaluates the limit cycle offset function using the experimental Hirata robot having position dependent variables. Figure 10 shows a steady state limit cycle for a position pointing step response of 0.001 radians using a PID + impulse hybrid controller. The mean peak to peak displacement of the smallest non-elastic part of the limit cycle is μ_d .

The experiment was repeated using the limit cycle offset function with the same position step reference of 0.001 radians. Figure 11 shows a sample experiment and in this example, the limit cycle offset function is activated at $t=0.9s$. At this time, the amplitude of the non elastic part of the limit cycle is identified as lying between the switching bounds. The switching bounds and dead-zone are set according to the methodology given earlier. Once the offset function is activated, the controller adjusts itself by forcing the proceeding pulse to be one increment wider before returning to the smallest pulse width. This results in the limit cycle being shifted down into the dead-zone region where the impulse controller is automatically disabled at $t=0.95s$. At this time, the final error is guaranteed to fall within the error dead zone which can be seen from Fig 11 to be in the vicinity of $\pm 1e-4$ radians.

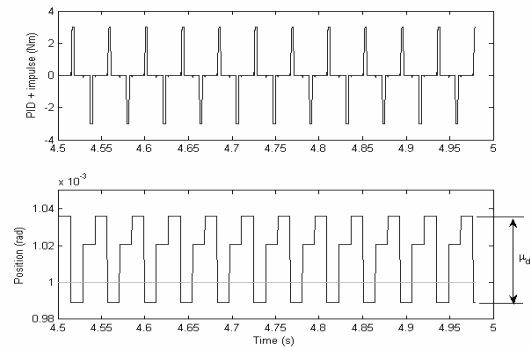


Figure 10: Steady state limit cycle for the PID + impulse hybrid controller when applying a unit step input to the Hirata robot. The mean peak to peak displacement μ_d is the non-elastic part of limit cycle.

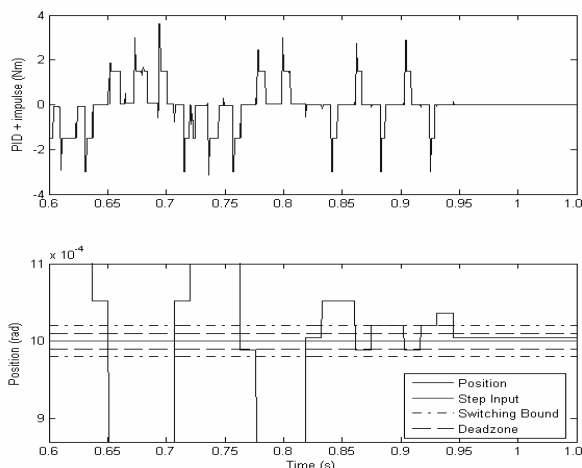


Figure 11: Using the 'Limit Cycle Offset' function to reduce the final steady state error of the Hirata robot.

4.2 Discussion of Results

This set of results demonstrates the Limit Cycle Offset function can be successfully applied to a commercial robot manipulator having characteristics of high non-linear friction. The results show that the unmodified controller will cause the robot to limit cycle near steady state position and that the peak to peak displacement is equal to the displacement of the smallest usable width pulse.

By using the Limit Cycle Offset function, the limit cycle can be detected and the pulse width adjusted so that at least one of the peaks of the limit cycle is moved towards the reference set point. Finally, the results show that the controller recognises the limit cycle as being shifted into a defined error dead-zone whereby the controller is disabled. The steady state error is therefore guaranteed to fall within a defined region so that the steady state error is reduced. For the SCARA robot, the improvement in accuracy demonstrated was 1.1×10^{-4} radians in comparison to 4.5×10^{-4} radians achieved without the limit cycle offset.

5 CONCLUSION

Advances in digital control have allowed the power electronics of servo amplifiers to be manipulated in a way that will improve a servomechanism precision without modification to the mechanical plant. This is particularly useful for systems having highly non-

linear friction where conventional control schemes alone under perform. A previously developed hybrid PID + Impulse controller which does not require the mechanism to come to a complete stop between pulses has been modified to further improve accuracy. This modification shifts the limit cycling into a different position to provide substantial additional improvement in the mechanism's position accuracy. This improvement has been demonstrated both in simulations and in experimental results on a SCARA robot arm. The mechanism does not have to come to a complete stop between pulses, and no mechanical modification has to be made to the robot.

REFERENCES

- Armstrong-Hélouvy, B., 1991, "Control of Machines with Friction" Kluwer Academic Publishers, 1991, Norwell MA.
- Armstrong-Hélouvy, B., Dupont, P., and Canudas de Wit, C., 1994, "A survey of models, analysis tools and compensation methods for the control of machines with friction" *Automatica*, vol. 30(7), pp. 1083-1138.
- Canudas de Wit, C., Olsson, H., Åström, K. J., 1995 "A new model for control of systems with friction" *IEEE Transactions on Automatic Control*, vol. 40 (3), pp. 419-425.
- Dahl, P., 1968, "A solid friction model" Aerospace Corp., El Segundo, CA, Tech. Rep. TOR-0158(3107-18)-1.
- Dahl, P., 1977, "Measurement of solid friction parameters of ball bearings" Proc. of 6th annual Symp. on Incremental Motion, *Control Systems and Devices*, University of Illinois, ILO.
- Hojjat, Y., and Higuchi, T., 1991 "Application of electromagnetic impulsive force to precise positioning" *Int J. Japan Soc. Precision Engineering*, vol. 25 (1), pp. 39-44.
- Johannes, V. I., Green, M.A., and Brockley, C.A., 1973, "The role of the rate of application of the tangential force in determining the static friction coefficient", *Wear*, vol. 24, pp. 381-385.
- Johnson, K.L., 1987, "Contact Mechanics" Cambridge University Press, Cambridge.
- Kato, S., Yamaguchi, K. and Matsubayashi, T., 1972, "Some considerations of characteristics of static friction of machine tool slideway" *J. o Lubrication Technology*, vol. 94 (3), pp. 234-247.
- Li, Z, and Cook, C.D., 1998, "A PID controller for Machines with Friction" Proc. Pacific Conference on Manufacturing, Brisbane, Australia, 18-20 August, 1998, pp. 401-406.
- Olsson, H., 1996, "Control Systems with Friction" Department of Automatic Control, Lund University, pp.46-48.
- Popovic, M.R., Gorinevsky, D.M., Goldenberg, A.A., 2000, "High precision positioning of a mechanism with non linear friction using a fuzzy logic pulse

- controller” *IEEE Transactions on Control Systems Technology*, vol. 8 (1) pp. 151-158.
- Rabinowicz, E., 1958, “The intrinsic variables affecting the stick-slip process,” *Proc. Physical Society of London*, vol. 71 (4), pp.668-675.
- Rathbun, D., Berg, M. C., Buffinton, K. W., 2004, “Piecewise-Linear-Gain Pulse Width Control for Precise Positioning of Structurally Flexible Systems Subject to Stiction and Coulomb Friction”, *ASME J .of Dynamic Systems, Measurement and Control*, vol. 126, pp. 139-126.
- Richardson, R. S. H., and Nolle, H., 1976, “Surface friction under time dependant loads” *Wear*, vol. 37 (1), pp.87-101.
- Wu, R., Tung, P., 2004, “Fast Positioning Control for Systems with Stick-Slip Friction”, *ASME J .of Dynamic Systems, Measurement and Control*, vol. 126, pp. 614-627.
- Yang, S., Tomizuka, M., 1988, “Adaptive pulse width control for precise positioning under the influence of stiction and Coulomb friction” *ASME J .of Dynamic Systems, Measurement and Control*, vol. 110 (3), pp. 221-227.



SciTeP Press
Science and Technology Publications